

Published in final edited form as:

Neuroscience. 2010 May 19; 167(3): 786–798. doi:10.1016/j.neuroscience.2010.02.037.

VOLTAGE-ACTIVATED CALCIUM CHANNEL EXPRESSION PROFILES IN MOUSE BRAIN AND CULTURED HIPPOCAMPAL NEURONS

B. SCHLICK, B. E. FLUCHER*, and G. J. OBERMAIR*

Department of Physiology and Medical Physics, Innsbruck Medical University, Fritz-Pregl-Strasse 3, A-6020 Innsbruck, Austria

Abstract

The importance and diversity of calcium signaling in the brain is mirrored by the expression of a multitude of voltage-activated calcium channel (Ca_V) isoforms. Whereas the overall distributions of α_1 subunits are well established, the expression patterns of distinct channel isoforms in specific brain regions and neurons, as well as those of the auxiliary β and $\alpha_2\delta$ subunits are still incompletely characterized. Further it is unknown whether neuronal differentiation and activity induce changes of Ca_V subunit composition. Here we combined absolute and relative quantitative TaqMan reverse transcription PCR (RT-PCR) to analyze mRNA expression of all high voltage-activated Ca_V α_1 subunits and all β and $\alpha_2\delta$ subunits. This allowed for the first time the direct comparison of complete Ca_V expression profiles of mouse cortex, hippocampus, cerebellum, and cultured hippocampal neurons. All brain regions expressed characteristic profiles of the full set of isoforms, except Ca_V1.1 and Ca_V1.4. In cortex development was accompanied by a general down regulation of α_1 and $\alpha_2\delta$ subunits and a shift from β_1/β_3 to β_2/β_4 . The most abundant Ca_V isoforms in cerebellum were Ca_V2.1, β_4 , and $\alpha_2\delta$ -2, and in hippocampus Ca_V2.3, β_2 , and $\alpha_2\delta$ -1. Interestingly, cultured hippocampal neurons also expressed the same Ca_V complement as adult hippocampus. During differentiation specific Ca_V isoforms experienced up- or down-regulation; however blocking electrical activity did not affect Ca_V expression patterns. Correlation analysis of α_1 , β and $\alpha_2\delta$ subunit expression throughout all examined preparations revealed a strong preference of Ca_V2.1 for β_4 and $\alpha_2\delta$ -2 and vice versa, whereas the other α_1 isoforms were non-selectively expressed together with each of the other β and $\alpha_2\delta$ isoforms. Together our results revealed a remarkably stable overall Ca²⁺ channel complement as well as tissue specific differences in expression levels. Developmental changes are likely determined by an intrinsic program and not regulated by changes in neuronal activity.

Keywords

VGCC; Ca²⁺; realtime RT-PCR; beta; alpha(2)delta; mRNA distribution

Voltage-activated Ca²⁺ channels (Ca_V) control multiple neuronal functions including transmitter release, gene transcription, and synaptic plasticity (Catterall, 2000). High voltage-activated Ca_Vs are heteromultimers consisting of a pore-forming α_1 and the auxiliary $\alpha_2\delta$ and β subunits (Catterall et al., 2005). Seven genes encode for α_1 subunits of L-type (Ca_V1.1 to Ca_V1.4) and non L-type (Ca_V2.1 to Ca_V2.3) channels, and four genes for each of the auxiliary β and $\alpha_2\delta$ subunits (Dolphin, 2003; Davies et al., 2007). Most of the

subunit isoforms are expressed in the central nervous system (Ludwig et al., 1997; Dolphin, 2003; Davies et al., 2007).

The L-type channels $\text{Ca}_V1.2$ and $\text{Ca}_V1.3$ perform primarily postsynaptic functions in transcriptional regulation and synaptic plasticity, whereas the non-L-type channels ($\text{Ca}_V2.1$, $\text{Ca}_V2.2$, $\text{Ca}_V2.3$) are responsible for neurotransmitter release. While some peripheral neurons, like superior cervical ganglion cells, are known to express only one presynaptic channel (Mochida et al., 2003), it is evident that the majority of brain regions and neurons express the whole plethora of Ca_V s (Vacher et al., 2008). Considering the additional diversity of the auxiliary subunits and the fact that all α_1 subunits seem to be capable of assembling with all β and $\alpha_2\delta$ isoforms, the complexity of possible subunit compositions becomes enormous. For example three distinct presynaptic Ca_V2 α_1 isoforms plus three $\alpha_2\delta$ and four β subunits already give 36 possible channel compositions; and that is without including the splice variants existing for all of the isoforms.

In light of this subunit diversity specific mechanisms must exist to assemble distinct $\alpha_1/\beta/\alpha_2\delta$ complexes in neurons. The simplest possible mechanism is to limit the number of isoforms expressed in a single cell at a given time. This is the case in skeletal muscle ($\text{Ca}_V1.1/\beta_{1a}/\alpha_2\delta-1$), cardiac myocytes ($\text{Ca}_V1.2/\beta_2/\alpha_2\delta-1$), and retina photoreceptor cells ($\text{Ca}_V1.4/\beta_2/\alpha_2\delta-4$) (Mori et al., 1991; Ball et al., 2002; Barnes and Kelly, 2002; Arikath and Campbell, 2003; Wycisk et al., 2006). Similarly, the cerebellum shows a strong preference towards one subunit combination ($\text{Ca}_V2.1/\beta_4/\alpha_2\delta-2$) (Ludwig et al., 1997; Brodbeck et al., 2002). In contrast, the cerebral cortex shows a more heterogenous expression of Ca_V isoforms (Ludwig et al., 1997; Klugbauer et al., 1999). Existing evidence from electrophysiological, pharmacological, and immunostaining experiments indicates that these narrow and broad expression patterns in cerebellum and cortex respectively, are also reflected in the α_1 subunit expression of specific types of neurons, like cerebellar granule cells and hippocampal pyramidal cells (Hell et al., 1993; Lorenzon and Foehring, 1995; Randall and Tsien, 1995; Westenbroek et al., 1995). However, little to no quantitative comparable data exist on the expression of Ca_V isoforms in different brain tissues and cells, and information on expression patterns of auxiliary subunits is sparse.

To bring more clarity into this complex situation we employed TaqMan quantitative RT-PCR (qRT-PCR) to measure the mRNA expression of all seven high voltage-activated Ca_V α_1 , and each of the four β and $\alpha_2\delta$ subunit genes. The generation of standard curves enabled the quantitative comparison of the transcript levels between the individual genes, and a rigorous normalization to endogenous reference genes allowed the direct comparison of the expression levels in mouse cortex, hippocampus, cerebellum, and cultured hippocampal neurons. All examined tissues and cells expressed the full complement of subunit isoforms, with the exception of $\text{Ca}_V1.1$ and $\text{Ca}_V1.4$. Characteristic developmental changes in the Ca_V subunit expression were evident in brain regions and cultured neurons. However, alteration of the electrical activity of cultured hippocampal neurons did not affect the Ca_V expression patterns. Together these data emphasize the great complexity of Ca_V expression in brain as well as in hippocampal pyramidal cells, and indicate a limited role of differential expression in controlling the subunit and isoform composition in neurons.

EXPERIMENTAL PROCEDURES

RNA isolation from cultured hippocampal neurons

Low-density cultures of hippocampal neurons were prepared from 16.5-day-old embryonic BALB/c mice as described (Obermair et al., 2003; Kaeck and Banker, 2006). Briefly, dissected hippocampi were dissociated by trypsin treatment and trituration. Neurons were plated on poly-L-lysine-coated glass coverslips at a density of 7000 cells/cm². After plating,

cells were allowed to attach for 3–4 h before transferring the coverslips neuron-side-down into 60-mm culture dishes with a glial feeder layer. Neurons and glial feeder layer were cultured in serum-free neurobasal medium (Invitrogen GmbH, Karlsruhe, Germany) supplemented with Glutamax and B27 supplements (Invitrogen GmbH). Five or 24 days after plating coverglasses with neurons were removed from the dishes with glia cells, harvested by trypsin treatment, and homogenized using QiaShredder columns (Qiagen, GmbH, Hilden, Germany). Total RNA was extracted using the RNeasy Protect Mini Kit (Qiagen, GmbH, Hilden, Germany). Reverse transcription was performed on 5 μ l of RNA using Superscript II reverse transcriptase (Invitrogen, Carlsbad, USA) and random hexamer primers (Promega, Madison WI, USA); the RT mix was incubated at 37 °C for 60 min.

RNA isolation from tissue

BALB/c mice of different age (E16, PD1, 2 and 8 weeks) were euthanized by CO₂ exposure and decapitated. From each mouse total RNA was isolated from the entire cerebral hemispheres (referred to as cortex), the hippocampus, and the cerebellum. To this end the skull was opened from caudal to rostral and the brain was carefully removed and placed in ice cold Hank's buffered salt solution. The entire cerebral hemispheres were isolated by separation from the diencephalon. The hippocampus was removed from one hemisphere using fine scissors. Next the entire cerebellum was cut from the brainstem. The respective tissues were further cut in four to six pieces and immediately transferred into RNAlater RNA Stabilization Reagent (Qiagen, GmbH, Hilden, Germany). Tissue samples were disrupted by using a rotor-stator homogenizer (Ultraturrax T8, IKA, Staufen, Germany) and QiaShredder columns. Total RNA was extracted from homogenized brain tissue using the RNeasy Protect Mini Kit (Qiagen, GmbH, Hilden, Germany). RNA concentrations were determined photometrically. Reverse transcription was performed on 1 μ g of RNA using Superscript II reverse transcriptase (Invitrogen, Carlsbad CA, USA) and random hexamer primers (Promega, Madison WI, USA); RT mix was incubated for 60 min at 37 °C. Animal handling was in accordance with national and international standards of animal welfare.

Quantitative real time PCR

The relative abundance of different Ca_v subunit transcripts was assessed by TaqMan qRT-PCR using a standard curve method based on PCR products of known concentration. TaqMan gene expression assays (Table 1), designed to span exon–exon boundaries, were purchased from Applied Biosystems (Foster City, CA, USA). For each assay, flanking primer pairs (Eurofins MWG Operon, Ebersberg, Germany) were designed to amplify templates for the standard curves using cDNA from mouse whole brain (Table 2). PCR products were separated on 1.5% low melting point agarose gels (Amresco, Solon, OH, USA). Bands were excised, DNA was extracted using Nucleospin Extract II columns (Macherey-Nagel, Düren, Germany) and sequenced (Eurofins MWG Operon Sequencing Department, Martinsried, Germany) to confirm the integrity of the obtained fragments. Concentrations of PCR products were determined using Quant-IT PicoGreen dsDNA Assay Kit (Invitrogen). Standard curve dilution series ranging from 10¹ to 10⁷ DNA molecules were generated in water containing 1 μ g/ml of poly-dC-DNA (Midland, TX, USA). qRT-PCRs of the standard curve samples were performed in triplicates and samples without template (background) served as negative controls. In order to determine standard reliability all standard curves were repeated two to three times (including all steps, see above) over the course of 2 years. Finally, average linear regressions were calculated for the combined results of all standard curve replicates. Only data points in the logarithmic amplification range of the respective standard curve were included for regression analysis. The limits of detection (LOD) and quantification (LOQ) of each TaqMan assay were obtained by subtracting 3 and 10 times, respectively, the root mean squares of the residuals, including background values, from the cycle threshold (Ct) value of the Y-intercept (Table 3) (Corley,

2003). In cases where assays did not show background Ct values or the spread of the background Ct values was large, LOQ was determined by subtracting 10 times the root mean squares of the residuals, excluding background, from the Ct value of the Y-intercept (Table 3). All standard curve data were included for this analysis.

qRT-PCR (50 cycles) was performed in duplicates using 20 ng total RNA equivalents of cDNA and the specific TaqMan gene expression assay for each 20 μ l reaction in TaqMan Universal PCR Master Mix (Applied Biosystems). Measurements were performed on at least three independent RNA preparations from each tissue and developmental stage. Analyses were performed using the 7500 Fast System (Applied Biosystems).

Endogenous controls and data normalization

To compare the relative expression of distinct Ca_v subunits in different preparations, data were normalized based on the most stable control gene determined as previously described (Vandesompele et al., 2002). The endogenous control genes included were [name (gene symbol), assay ID (Applied Biosystems)]: β -cytoplasmic actin (ACTB), Mm00607939_s1; beta-2-microglobulin (B2M), Mm00437762_m1; glyceraldehyde-3-phosphate dehydrogenase (GAPD), Mm99999915_g1; hypoxanthine phosphoribosyl-transferase 1 (HPRT1), Mm00446968_m1; succinate dehydrogenase complex, subunit A (SDHA), Mm01352363_m1; tata box binding protein (TBP), Mm00446973_m1; transferrin receptor (TFRC), Mm00441941_m1. HPRT1 and SDHA were determined to be the most stably expressed reference genes when comparing all preparations (Suppl. 1). The Ct values for each Ca_v gene expression assay were recorded for each individual preparation. To allow a direct comparison between the expression levels in different tissues, we normalized all experiments to the Ct value of HPRT1 in the RNA preparation yielding the highest HPRT1 Ct value. Subsequently, normalized molecule numbers were calculated for each Ca_v subunit from their respective standard curve. For determining the number of molecules per neuron (see below), molecule numbers were calculated from the raw Ct values.

Estimating the number of transcript molecules per cultured neuron

To estimate the number of transcript molecules of each Ca_v subunit we first determined the number of neurons per coverslip. Coverslips of four 24 DIV hippocampal cultures were stained with Hoechst dye to distinguish nuclei and analyzed on an Axiovert 200M microscope (Carl Zeiss GmbH, Wien, Austria) using a 10 \times objective. The number of neurons per coverslip was extrapolated to the total number of neurons per RNA preparation and RT reaction and, finally, to the amount of RNA equivalents used for the qRT-PCR reaction.

Data analysis and statistics

Data were organized and analyzed using MS Excel and SPSS statistical software (SPSS Inc., Chicago, IL, USA) as indicated. Statistical significance was determined by Student's *t*-test and ANOVA. To correct for multiplicity in analyses involving many pairwise comparisons the Holm procedure (Bonferroni step-down correction) was applied (Bender and Lange, 2001). After Holm correction *P*-values <0.05 were considered as statistically significant. All data are presented as mean \pm SE for the indicated number of experiments. Graphs and figures were generated using MS Excel, Origin 7, and Adobe Photoshop 8.0 software.

RESULTS

Ca_v expression profiles of mouse hippocampus, cortex, and cerebellum

Previous studies demonstrated the existence of mRNA and protein of Ca_v α_1 (Ca_v1.2, Ca_v1.3, Ca_v2.1, Ca_v2.2, and Ca_v2.3), $\alpha_2\delta$ ($\alpha_2\delta$ -1, $\alpha_2\delta$ -2, $\alpha_2\delta$ -3), and of all four β subunits

in the mammalian brain (for review see Catterall, 2000; Arikath and Campbell, 2003). Nevertheless, quantitatively comparable expression levels of the distinct Ca_V subunit isoforms in different brain regions of a single mammalian species were missing. One reason being the inherent difficulty to quantitatively compare the outcomes of methods based on different antibodies, riboprobes, or PCR primers. Quantitative TaqMan RT-PCR analysis is the state-of-the-art approach to analyze relative mRNA amounts in distinct probes, provided a suitable and stably expressed reference gene has been identified. Moreover, the quantitative comparison of the expression level of different genes is hampered by variations in the sensitivities and amplification kinetics of the various qRT-PCR assays. Therefore we combined relative quantification based on endogenous control genes with absolute quantification based on individual standard curves. This allowed us to determine the amount of each Ca_V isoform transcript in different mouse brain regions and cultured hippocampal neurons, and to get an accurate estimate on the quantities of each transcript relative to each other.

Hippocampus, cortex, and cerebellum of adult (8 weeks old) mice expressed all high voltage-activated Ca_V α_1 subunits, except the skeletal muscle $\text{Ca}_V1.1$ and the retinal $\text{Ca}_V1.4$, which were expressed at ~ 1000 -fold lower levels, around the limit of quantification (Fig. 1A). Furthermore, all four β subunit genes and three of the four $\alpha_2\delta$ subunit genes were robustly expressed in these brain tissues (Fig. 1B, C). $\alpha_2\delta-4$ molecule numbers were above the limit of quantification in all qRT-PCR runs. However, when compared to the other auxiliary subunits its expression levels were negligible. Overall, the L-type channels ($\text{Ca}_V1.2$ and $\text{Ca}_V1.3$) were expressed at lower levels than each of the non-L-type channels ($\text{Ca}_V2.1$, $\text{Ca}_V2.2$, and $\text{Ca}_V2.3$). Whereas the expression profile was fairly similar between cortex and hippocampus, cerebellum showed some striking differences. $\text{Ca}_V2.1$, β_4 , and $\alpha_2\delta-2$ were the dominating isoforms in cerebellum and were expressed two to threefold higher compared to cortex and hippocampus (Fig. 1A–C). The high expression of these three Ca_V isoforms in the cerebellum confirms previous findings (Ludwig et al., 1997; Hobom et al., 2000; Barclay et al., 2001; Cole et al., 2005) and thus strengthens the confidence in our new quantification method. Cerebellar expression levels of L-type channels also differed from those in the other two brain regions in that the ratio of $\text{Ca}_V1.2$ to $\text{Ca}_V1.3$ was 4:1 in cerebellum, whereas it was $\sim 1:1$ in cortex and hippocampus. Our observation that $\text{Ca}_V1.3$ transcripts accounted for only $\sim 20\%$ of cerebellar L-type channels is again consistent with previous observations (Koschak et al., 2007; Sinnegger-Brauns et al., 2009). Moreover, whereas $\alpha_2\delta-1$ was the dominating $\alpha_2\delta$ subunit isoform in cortex and hippocampus, this isoform was markedly reduced in the cerebellum (Fig. 1C). Unexpectedly the $\text{Ca}_V2.3$ and β_2 mRNAs were twofold higher in the hippocampus than in cortex and cerebellum. Actually they were the highest expressed α_1 and β isoforms in the hippocampus. Finally, the expression of $\text{Ca}_V2.2$ and $\alpha_2\delta-3$ was remarkably uniform throughout the three brain regions.

Ca_V expression patterns change during development

Because Ca_V s have been previously demonstrated to be important for neuronal maturation and development (Pravettoni et al., 2000; Splawski et al., 2004), we next sought to investigate whether and how their expression patterns change from late embryonic until adult stages. To this end we analyzed the expression profiles on embryonic day 16 (E16), postnatal day 1 (PD1), and at 2 weeks and 8 weeks of age (Fig. 2). In line with the expression profiles of 8 weeks old mice (Fig. 1), $\text{Ca}_V1.1$ and $\text{Ca}_V1.4$ were absent from both tissues at all time points (Fig. 2A, B). In cortex three different patterns of developmental changes could be observed (Fig. 2A): the majority of isoforms showed decreasing expression levels ($\text{Ca}_V1.2$, $\text{Ca}_V2.2$, $\text{Ca}_V2.3$, β_1 , β_3 , $\alpha_2\delta-2$), four isoforms showed stable expression levels ($\text{Ca}_V1.3$, $\text{Ca}_V2.1$, $\alpha_2\delta-1$ and $\alpha_2\delta-3$), and the levels of two isoforms (β_2 and β_4) showed a significant increase with development. Interestingly, the total number of

Ca_v α_1 transcripts was about twofold larger in developing than in mature brain. A similar trend was observed for the $\alpha_2\delta$ subunits, but not for total β subunits. Individually, the β subunits showed very pronounced developmental changes. Whereas β_1 and β_3 levels declined as the majority of the α_1 subunits, β_2 and β_4 expression levels significantly increased. Thus, in contrast to the α_1 subunits, the total number of β subunit transcripts remained fairly constant during development. However, their ratio shifted from predominantly β_1 and β_3 in embryonic cortex, to mostly β_2 and β_4 in the mature cortex.

In the developing hippocampus (Fig. 2B) expression levels of many subunits showed the same tendency as in whole cortex. The most striking difference was the fact that Ca_v2.3 and β_1 levels did not show the developmental decline observed in cortex. The developmental increase of β_2 was even more pronounced whereas β_3 showed a dramatic drop within the short period between E16 and PD1. This drop was also observed in cortex (Fig. 2A). Surprisingly, in hippocampus expression of $\alpha_2\delta$ -4 increased ~20 fold during development, although still at a very low level.

Cultured hippocampal neurons express the same subunit isoforms as adult hippocampus

The overall Ca_v expression profile in hippocampus, cortex, and cerebellum represents the sum of RNAs derived from a large number of different neuronal and non-neuronal cell types. As a consequence, developmental changes may indicate an overall change in all cells, or it may result from manifold greater changes in subpopulations of cells. On the other hand, a decline of a specific transcript in one cell type might coincide with an increase of the same transcript in another cell type and thus mask the developmental change. Therefore, in addition to understanding the overall Ca_v channel expression patterns in brain and distinct brain regions, it is vitally important to understand the subunit expression in single types of neurons. Low density cultured hippocampal neurons serve as an ideal model to address this question. First, this cell culture system is a pure neuronal culture without glia. Second, it represents a highly homogenous culture with >90% glutamatergic pyramidal cells (Benson et al., 1994; Obermair et al., 2003). In light of this it is remarkable that qRT-PCR analysis revealed the same set of Ca_v subunit isoforms in differentiated cultured hippocampal neurons (24 DIV) as in adult hippocampus expressed (Fig. 3). This indicates that the complexity of Ca_v expression pattern exists in individual neuron types also and does not only arise from a mix of different cell types with distinct sets of calcium channels. Interestingly, with one exception (Ca_v2.3) the expression levels of the α_1 isoforms were similar to those in hippocampus (Fig. 3A). Transcript levels of Ca_v2.3 in the culture were much lower than in hippocampus. In the culture Ca_v2.1 was the most abundant α_1 subunit. Similar to Ca_v2.3, β_2 and $\alpha_2\delta$ -1 (and to a lesser degree also β_1 and β_4) showed substantially lower expression levels in hippocampal neurons than in whole hippocampus. Consequently the hippocampus-specific expression profile of the auxiliary subunits was not observed in the cultured neurons, but β_1 to β_4 and $\alpha_2\delta$ -1 to $\alpha_2\delta$ -3 were all expressed at approximately equal amounts (Fig. 3B, C).

Specific developmental upregulation of Ca_v2.1 and $\alpha_2\delta$ -2 in cultured hippocampal neurons

Cultured hippocampal neurons undergo dramatic morphological changes during growth and differentiation *in vitro*. The first week is characterized by massive neurite outgrowth. While first synapses appear around 3 DIV, the maturation of the dendritic tree starts around 5–7 DIV. In the following weeks the neurons develop a large and elaborate dendritic tree with numerous dendritic spines and an increasing number of synapses (Fletcher et al., 1994; Obermair et al., 2003). Interestingly, during this period of continuous differentiation from 5 DIV to 24 DIV most Ca_v subunit isoforms showed only a slight increase or remained expressed at constant levels (Fig. 4A). The notable exceptions were the P/Q-type channel Ca_v2.1 and the $\alpha_2\delta$ -2 subunit, both of which experienced a significant up-regulation.

Among the β subunits β_4 showed the strongest increase. In contrast, expression levels of $\text{Ca}_v2.3$ and $\alpha_2\delta-1$ decreased during the same time frame.

Blocking neuronal activity does not alter the Ca_v expression pattern in cultured hippocampal neurons

Neurons adapt to alterations in the activity status and synaptic transmission by homeostatic plasticity (Turrigiano, 2008). Decreasing overall activity generally leads to an increase in the cellular excitability, whereas increased activity leads to a decrease therein. These homeostatic alterations are caused by both presynaptic and postsynaptic adaptations also involving gene transcription. Because Ca_v s are major constituents of both pre- and postsynaptic compartments and are indirectly (Deisseroth et al., 2003; Dolmetsch, 2003) and likely also directly (Gomez-Ospina et al., 2006; Subramanyam et al., 2009) involved in the regulation of transcription, we tested whether their expression patterns change upon blocking neuronal activity. Well differentiated cultured hippocampal neurons display robust spontaneous activity, which can be suppressed by tetrodotoxin (TTX) or further increased by blocking inhibitory input with bicuculline (Harms and Craig, 2005; Turrigiano and Nelson, 2004). Surprisingly, overnight application of TTX did not affect the expression level of any Ca_v subunit isoforms (Fig. 4B) although the same experimental paradigm induced the nuclear translocation of the $\text{Ca}_v \beta_{4b}$ subunit (Subramanyam et al., 2009). N-methyl-D-aspartate (NMDA) receptors are critically involved in the control of plasticity-related gene expression and long-term memory formation (e.g. Jordan and Kreutz, 2009), and blockage by DL-2-amino-5-phosphonopentanoic acid (DL-AP5) leads to a local increase of synaptic NMDA receptors without inducing overall homeostatic changes (Rao and Craig, 1997; Obermair et al., 2003; Turrigiano, 2008). However, also chronic blockage of NMDA receptors did not change the Ca_v expression profile (Suppl. 2).

DISCUSSION

This is the first study providing a comprehensive calcium channel expression profile of mouse brain and cultured hippocampal neurons. This study is unique in that it quantifies the expression of the full complement of high voltage-activated calcium channels α_1 together with all $\alpha_2\delta$ and β subunits, and in that for the first time this quantification is thoroughly based on a quantitative assessment of the underlying assay variability, thus allowing a direct comparison of expression levels between all isoforms and across multiple preparations.

The Ca_v transcriptome of mouse brain regions and cultured hippocampal neurons

Comparing the calcium channel expression profiles of cortex, hippocampus, and cerebellum revealed expression of the same complement of Ca_v isoforms. Overall, expression of L-type calcium channels was lower than that of non-L-type channels, both individually and in sum. $\text{Ca}_v1.2$ and $\text{Ca}_v1.3$ were the only L-type calcium channels expressed in mouse brain. In the cerebellum they were found at a ratio of 4:1 ($\text{Ca}_v1.2$: $\text{Ca}_v1.3$), which is consistent with results from previous dihydropyridine binding studies and qRT-PCR analysis (Koschak et al., 2007; Sinnegger-Brauns et al., 2009). In cortex and hippocampus $\text{Ca}_v1.2$ and $\text{Ca}_v1.3$ were expressed at equal levels. Generally this is in agreement with published data on the relative L-type Ca_v distribution in different rat and mouse brain regions (Qin et al., 2002; Doering et al., 2007; Sinnegger-Brauns et al., 2009). However, we found no evidence for the expression relatively high levels of $\text{Ca}_v1.1$ mRNA that has been reported in a study on human brain (Takahashi et al., 2003). Thus, our expression profile confirms previous data on the expression of L-type calcium channels in the brain, and it adds the new finding that, at least in some species or mouse strains, levels of $\text{Ca}_v1.3$ mRNA in the cortex and hippocampus can be as high as those of $\text{Ca}_v1.2$. This is important in light of their distinct

roles in the formation of long term memory (Moosmang et al., 2005) and the involvement of Ca_v1.3 in depression (Busquet et al., 2009).

In the family of the non-L-type calcium channels, we observed the expected high levels of Ca_v2.1 in the cerebellum. Ca_v2.1 was also the highest expressed α_1 subunit in the cortex. In hippocampus however, Ca_v2.3 was expressed at twice the levels found in cortex and cerebellum, and thus was the dominant Ca_v isoform. Ca_v2.3 has been shown to be involved in presynaptic transmitter release in calyx-type terminals in the trapezoid body (Wu et al., 1998, 1999) and in presynaptic LTP in mossy fiber synapses (Dietrich et al., 2003). Postsynaptically, Ca_v2.3 is a major contributor to action potential evoked calcium transients in dendritic spines and is involved in postsynaptic plasticity (Yasuda et al., 2003). The high expression levels observed here may correspond to this twofold role in hippocampal neurons. Interestingly, hippocampal neurons in culture, which consist of mostly pyramidal cells, did not show similarly prominent Ca_v2.3 expression levels (cf. Fig. 3A).

Each of the four β subunits and three of the four $\alpha_2\delta$ subunits were expressed in all examined brain regions. The tissue-specific prevalence of Ca_v2.1 in cerebellum was paralleled by high expression of β_4 and $\alpha_2\delta-2$. This is consistent with previous results of a Western blot and *in situ* hybridization study (Ludwig et al., 1997), as well as with the similarity of phenotypes reported for mutant mice of Ca_v2.1 (tottering, leaner), β_4 (lethargic), and $\alpha_2\delta-2$ (ducky and entla) (Burgess et al., 1997; Doyle et al., 1997; Barclay et al., 2001; Brill et al., 2004). In hippocampus β_2 and $\alpha_2\delta-1$ were the highest expressed auxiliary subunits. Based on experiments involving specific β_2 riboprobes and antibodies (Ludwig et al., 1997; Day et al., 1998; Pichler et al., 1997) the overall high levels of β_2 transcripts in all brain regions was not to be expected. Because our β_2 TaqMan assay showed a comparably low sensitivity (high Ct values and standard curves), we reanalyzed selected samples with a second β_2 assay. This confirmed the high β_2 expression levels (data not shown). Apparently specific properties of the β_2 transcript, like the secondary structure, may render it less accessible to riboprobes and PCR primers. This would explain both, the previously reported low signals of *in situ* hybridization and the high raw Ct values observed in our own. Nevertheless, previous Western Blot experiments performed on rat and rabbit tissues still indicate a low β_2 subunit abundance in brain (Ludwig et al., 1997; Pichler et al., 1997).

The Ca_v expression profile in hippocampus reflects the sum of expression patterns in a variety of different neuronal and non-neuronal cells. Thus Ca_v expression of individual neuron types may differ greatly from the overall hippocampal profile. Therefore it was quite surprising to find that cultured hippocampal pyramidal cells express all the same Ca_v subunit isoforms as hippocampus, although the expression levels of all four β subunits and $\alpha_2\delta-1$ through $\alpha_2\delta-3$ were fairly uniform. Nevertheless, this expression profile is characteristic for cultured hippocampal neurons and distinct from Ca_v expression patterns in other differentiated neurons, like dorsal root ganglion or cerebellar granule neurons (Obermair et al., unpublished results). This suggests that in cultured hippocampal pyramidal cells, a restricted expression of auxiliary subunit isoforms is not the strategy to achieve specific Ca_v subunit compositions. Consequently specific targeting properties and interactions with anchoring proteins in pre- and postsynaptic compartments must be responsible for assembling channels with distinct subunit compositions (Obermair et al., 2010). One striking difference to hippocampus tissue was the reduction of Ca_v2.3, β_2 , and $\alpha_2\delta-1$ levels in hippocampal neurons. Either neurons other than pyramidal cells account for the prominent expression of these isoforms in the hippocampus, or transcriptional regulation in the hippocampus is strongly dependent on cell-cell interactions or trophic factors missing in the culture system.

Developmental changes of selected isoforms in brain and hippocampal neurons

In the weeks following birth expression of Ca_v1.2, Ca_v2.2, and Ca_v2.3 in the cortex experiences a dramatic decline, while transcript levels of Ca_v1.3 and Ca_v2.1 remain constant. Thus, 8 weeks after birth the quantity of total α_1 subunit mRNA is reduced to about half of that expressed in late embryonic development. Considering the numerous important functions of voltage-gated calcium channels in mature neurons this developmental drop is remarkable. Either Ca_vs play more important roles in developing neurons than so far anticipated, or upon differentiation the stabilization of Ca_vs in pre- and postsynaptic compartments reduces their turnover rate and thus high levels of protein expression may be maintained, even though transcription rates are reduced.

The fact that during this critical period, in which electrical activity sets in and synaptic connections are established, none of the α_1 subunits is up-regulated indicates that the pore-forming subunits do not undergo a developmental isoform switch. The same is true for the $\alpha_2\delta$ subunits. In contrast, developmental expression of the β subunits shows a marked isoform switch. Whereas β_1 and β_3 decline in parallel to the α subunits, expression of β_2 and β_4 experiences a significant increase, suggesting that calcium channels change their β subunit composition upon neuronal differentiation. The β isoform shift during neuronal differentiation is expected to result in a functional switch of calcium channels without actually changing the α_1 subunit. Furthermore, β subunits are essential for membrane expression of Ca_vs in heterologous cells as well as in neurons (Dolphin, 2003; Leroy et al., 2005; Obermair et al., 2008, 2010). At the late embryonic stage total α_1 transcripts are in excess of total β transcripts and around birth total expression of α_1 subunits declines, while total expression of β subunits remains constant. In fact, at 8 weeks after birth total α_1 and β transcript levels are nearly balanced. If the available amount of β subunits is limiting membrane expression of Ca_vs, the overall decline of functionally expressed Ca_v proteins may be smaller than indicated by the numbers of α_1 subunit transcripts.

In hippocampus developmental changes of Ca_v isoforms mirror those of cortex with one notable exception. Ca_v2.3 remains expressed at constantly high levels, thus becoming the predominant α_1 subunit isoform in mature hippocampus. Furthermore the developmental up-regulation of β_2 is more pronounced than that of β_4 . Together these changes give rise to the predominant expression levels of Ca_v2.3 and β_2 in the 8 weeks old hippocampus when compared to cortex (see Fig. 1A, B). *In vitro* differentiating cultured hippocampal neurons do not reflect the developmental changes observed in whole hippocampus. During the period when the cultured pyramidal cells differentiate into axons and dendrites and form numerous synaptic contacts, Ca_v2.3 declines, whereas expression of mainly presynaptic isoforms Ca_v2.1, $\alpha_2\delta$ -2, and β_4 increases. This observation is consistent with the dramatic increase in the synapse number (Obermair et al., 2003) and is consistent with a change in the channels coupled to glutamate release from mainly N-type channels to P/Q-type channels during *in vitro* development (Scholz and Miller, 1995).

Global changes in activity quickly induce synaptic scaling mechanisms involving gene-expression (Ibata et al., 2008), and activity-dependent regulation of membrane turnover of Ca_v1.2 expression has been suggested (Green et al., 2007). Therefore we examined whether the specific changes in Ca_v isoform expression observed during differentiation are activity dependent. Contrary to our expectation treating cultured hippocampal neurons with TTX or DL-AP5 did not result in any changes in Ca_v isoform expression. This indicates that the observed developmental changes in Ca_v expression in neurons may be intrinsically regulated, independent of electrical or synaptic activity.

Correlated expression of specific subunit isoforms

Recurring α_1 , β , and $\alpha_2\delta$ expression patterns in different samples or their coordinated up- and down-regulation can be indicative of the existence of preferential subunit combinations in neurons throughout the brain. Thus correlation analysis may be useful to suggest or exclude the existence of such preferential Ca_v complexes. Our correlation analysis is based on the following assumptions: (1) if Ca_v α_1 isoforms have a preference for specific auxiliary isoforms, or (2) if the expression of certain isoforms is co-regulated, and (3) if this preference or co-regulation is constant in different brain regions, cells and conditions, then this should be revealed in a correlation analysis. For example the correlation analysis (Fig. 5A) clearly identified the preference of Ca_v2.1 for β_4 and $\alpha_2\delta$ -2 subunits, reflecting their disproportional high expression in cerebellum and their concomitant up-regulation during development of hippocampal pyramidal cells. In tissues such a correlation could also arise from parallel but independent up- and down-regulation of these subunits in different cells. Therefore it is remarkable that a correlated up-regulation of the same subunits (Ca_v2.1, β_4 , and $\alpha_2\delta$ -2) could also be observed during the differentiation of cultured neurons (Fig. 5B). Within one cell type the most likely interpretation of a correlated up-regulation of Ca_v2.1, β_4 , and $\alpha_2\delta$ -2 is indeed that these subunit isoforms actually form a channel together.

Another striking upshot of the correlation analysis is the similarity of correlations between Ca_v1.2, Ca_v2.2 and Ca_v2.3. Expression of these α_1 subunits correlates positively with β_1 , β_3 , $\alpha_2\delta$ -1, and $\alpha_2\delta$ -3 (Fig. 5A). Interestingly, the same four auxiliary subunit isoforms correlate negatively with Ca_v2.1. During early development of the cortex all these channels and auxiliary subunits undergo a strong and concomitant down-regulation. The preference for the same auxiliary subunits may lead to a functional redundancy of Ca_v2.2 and Ca_v2.3 in supporting synaptic transmission. However, their differential expression in cortex and hippocampus suggests that Ca_v2.2 and Ca_v2.3 may be dominating in distinct cell types. The specific subunit combination Ca_v2.1/ β_4 / $\alpha_2\delta$ -2 on one side and a promiscuous association of Ca_v2.2 and Ca_v2.3 with any combination of β_1 , β_3 , $\alpha_2\delta$ -1, and $\alpha_2\delta$ -3 on the other side may explain why loss of Ca_v2.1 in null-mutant mice causes severe neurological disease (Jun et al., 1999), whereas loss of Ca_v2.2 or 2.3 results in little to no neurological phenotype (Saegusa et al., 2000; Ino et al., 2001).

Transcript numbers of individual neurons

Estimated transcript numbers of the different Ca_v subunit isoforms per cultured hippocampal neuron ranged from 0 to 12 (Table 4). The total number of transcripts per cell was 26 α_1 , 16 β , and 6 $\alpha_2\delta$ s. However, depending on the length of the reading frame a single transcript will yield different numbers of proteins per unit time. Assuming a maximal translation rate of 5 amino acids per second (Boehlke and Friesen, 1975) a single ribosome yields approximately 10 α_1 , 20 $\alpha_2\delta$, and 40 β proteins per hour. If we further assume that every transcript is occupied by 10 ribosomes (Mata et al., 2005), then our present data predict the translation of ~2600 α_1 , ~6400 β , and ~1200 $\alpha_2\delta$ molecules per hour and neuron. On the protein level our previous quantitative immunofluorescence analysis revealed that an average cultured hippocampal neuron may contain approximately 4000 Ca_v1.2 clusters, each consisting of eight channels on average (Obermair et al., 2004), in total ~32,000 proteins. With the translation rates estimated above, this corresponds to a complete turnover of the entire Ca_v1.2 complement in 64 h. Such protein turnover rates are slower than previously suggested membrane turnover rates based on TIRF analysis (Green et al., 2007), but are in line with estimated turnover rates of β subunits (Berrow et al., 1995) and the high stability of membrane expressed Ca_v1.2 clusters observed in hippocampal neurons (Di Biase et al., 2008). If Ca_v subunits in the neurons are associated at a 1:1:1 (α_1 : β : $\alpha_2\delta$) stoichiometry, these numbers suggest two- and fourfold higher β protein turnover rates compared with α_1 and $\alpha_2\delta$, respectively. On the other hand, additional free

auxiliary subunits might also be involved in functions independent of the Ca_v complex. This possibility is supported by the existence of a fraction of $\alpha_2\delta$ -2 subunits not associated with the channel complex (Davies et al., 2006), and the recent findings of a β_4 subunit located in nuclei of cerebellar neurons (Subramanyam et al., 2009).

CONCLUSION

Combining relative and absolute qRT-PCR quantification for the first time allowed the direct quantitative comparison of the Ca_v expression profile in different brain regions, cultured neurons, and treatment conditions. Our results clearly revealed a remarkably stable overall Ca²⁺ channel complement as well as tissue specific differences in expression levels. Furthermore we could show that low-density cultured hippocampal neurons, a widely used neuronal model system, express all the same Ca²⁺ channel subunit isoforms as adult hippocampus. Developmental changes are likely determined by an intrinsic program and not regulated by changes in neuronal activity. Interestingly, whereas correlation of expression patterns indicated a great permissiveness of interactions between α_1 and auxiliary subunits, Ca_v2.1 was different in that it showed a strong preference for β_4 and $\alpha_2\delta$ -2 subunits not only in cerebellum but also in hippocampal neurons.

Supplementary Material

Refer to Web version on PubMed Central for supplementary material.

Acknowledgments

We thank Gilda Pelster for technical assistance. This work was supported by grants from the Austrian Science Fund and the Austrian National Bank P17806-B05, P17807-B05, P20059-B05. This work is part of the PhD thesis of B.S.

APPENDIX

Supplementary data

Supplementary data associated with this article can be found, in the online version, at doi: 10.1016/j.neuroscience.2010.02.037.

Abbreviations

Ca_v	voltage-activated calcium channel
cDNA	complementary DNA
Ct	cycle threshold
DIV	days <i>in vitro</i>
DL-AP5	DL-2-amino-5-phosphonopentanoic acid
E16	embryonic day 16
HPRT1	hypoxanthine phosphoribosyl-transferase 1
LOD	limit of detection
LOQ	limit of quantification
mRNA	messenger RNA
NMDA	N-methyl-D-aspartate

PD1	postnatal day 1
qRT-PCR	quantitative reverse transcription PCR
TTX	tetrodotoxin

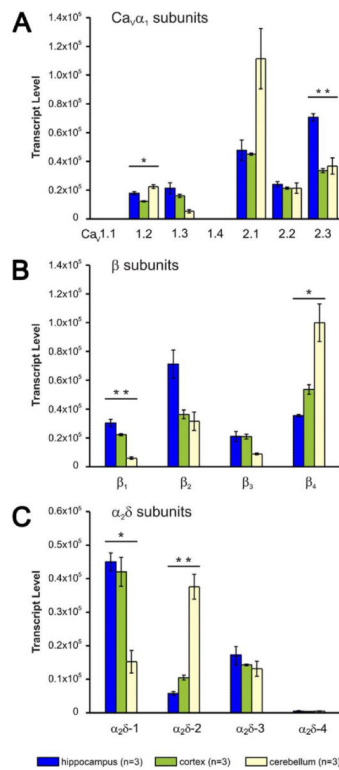
REFERENCES

- Arikkath J, Campbell KP. Auxiliary subunits: essential components of the voltage-gated calcium channel complex. *Curr Opin Neurobiol.* 2003; 13:298–307. [PubMed: 12850214]
- Ball SL, Powers PA, Shin HS, Morgans CW, Peachey NS, Gregg RG. Role of the beta(2) subunit of voltage-dependent calcium channels in the retinal outer plexiform layer. *Invest Ophthalmol Vis Sci.* 2002; 43:1595–1603. [PubMed: 11980879]
- Barclay J, Balaguero N, Mione M, Ackerman SL, Letts VA, Brodbeck J, Canti C, Meir A, Page KM, Kusumi K, Perez-Reyes E, Lander ES, Frankel WN, Gardiner RM, Dolphin AC, Rees M. Ducky mouse phenotype of epilepsy and ataxia is associated with mutations in the *Cacna2d2* gene and decreased calcium channel current in cerebellar Purkinje cells. *J Neurosci.* 2001; 21:6095–6104. [PubMed: 11487633]
- Barnes S, Kelly ME. Calcium channels at the photoreceptor synapse. *Adv Exp Med Biol.* 2002; 514:465–476. [PubMed: 12596939]
- Bender R, Lange S. Adjusting for multiple testing—when and how? *J Clin Epidemiol.* 2001; 54:343–349. [PubMed: 11297884]
- Benson DL, Watkins FH, Steward O, Banker G. Characterization of GABAergic neurons in hippocampal cell cultures. *J Neurocytol.* 1994; 23:279–295. [PubMed: 8089704]
- Berrow NS, Campbell V, Fitzgerald EM, Brickley K, Dolphin AC. Antisense depletion of beta-subunits modulates the biophysical and pharmacological properties of neuronal calcium channels. *J Physiol.* 1995; 482:481–491. [PubMed: 7537818]
- Boehlke KW, Friesen JD. Cellular content of ribonucleic acid and protein in *Saccharomyces cerevisiae* as a function of exponential growth rate: calculation of the apparent peptide chain elongation rate. *J Bacteriol.* 1975; 121:429–433. [PubMed: 1089627]
- Brill J, Klocke R, Paul D, Boison D, Gouder N, Klugbauer N, Hofmann F, Becker CM, Becker K. *entla*, a novel epileptic and ataxic *Cacna2d2* mutant of the mouse. *J Biol Chem.* 2004; 279:7322–7330. [PubMed: 14660671]
- Brodbeck J, Davies A, Courtney JM, Meir A, Balaguero N, Canti C, Moss FJ, Page KM, Pratt WS, Hunt SP, Barclay J, Rees M, Dolphin AC. The ducky mutation in *Cacna2d2* results in altered Purkinje cell morphology and is associated with the expression of a truncated alpha 2 delta-2 protein with abnormal function. *J Biol Chem.* 2002; 277:7684–7693. [PubMed: 11756448]
- Burgess DL, Jones JM, Meisler MH, Noebels JL. Mutation of the Ca^{2+} channel beta subunit gene *Cchb4* is associated with ataxia and seizures in the lethargic (lh) mouse. *Cell.* 1997; 88:385–392. [PubMed: 9039265]
- Busquet P, Khoi Nguyen N, Schmid E, Tanimoto N, Seeliger MW, Ben-Yosef T, Mizuno F, Akopian A, Striessnig J, Singewald N. *CaV1.3* L-type Ca^{2+} channels modulate depression-like behaviour in mice independent of deaf phenotype. *Int J Neuropsychopharmacol.* 2009; 11:1–15.
- Catterall WA. Structure and regulation of voltage-gated Ca^{2+} channels. *Annu Rev Cell Dev Biol.* 2000; 16:521–555. [PubMed: 11031246]
- Catterall WA, Perez-Reyes E, Snutch TP, Striessnig J. International Union of Pharmacology. XLVIII. Nomenclature and structure-function relationships of voltage-gated calcium channels. *Pharmacol Rev.* 2005; 57:411–425. [PubMed: 16382099]
- Cole RL, Lechner SM, Williams ME, Prodanovich P, Bleicher L, Varney MA, Gu G. Differential distribution of voltage-gated calcium channel alpha-2 delta (*alpha2delta*) subunit mRNA-containing cells in the rat central nervous system and the dorsal root ganglia. *J Comp Neurol.* 2005; 491:246–269. [PubMed: 16134135]

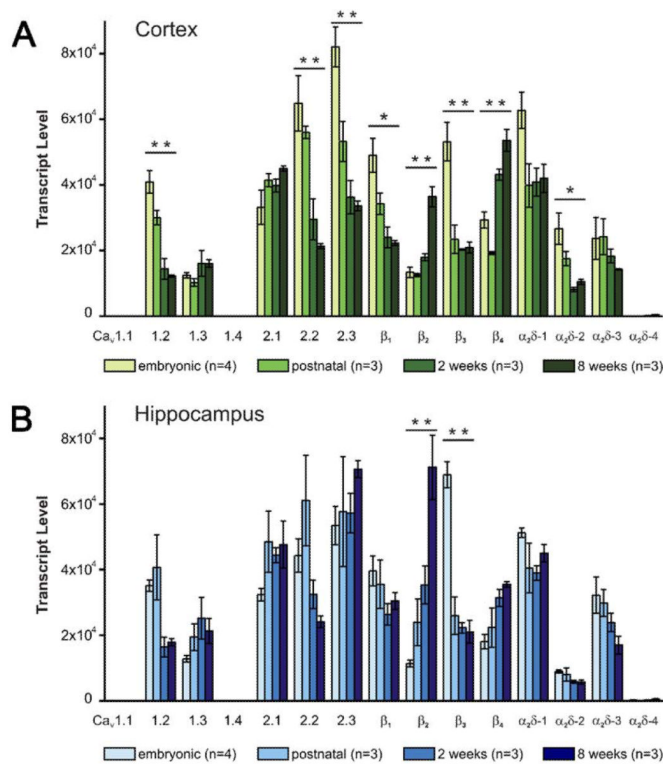
- Corley, J. Best practices in establishing detection and quantification limits for pesticide residues in foods. In: Lee, PW., editor. Handbook of residue analytical methods for agrochemicals. Vol. 1. John Wiley & Sons, Ltd; East Sussex, United Kingdom: 2003. p. 1-18. [LS0203]
- Davies A, Douglas L, Hendrich J, Wratten J, Tran Van Minh A, Foucault I, Koch D, Pratt WS, Saibil HR, Dolphin AC. The calcium channel $\alpha_2\delta_2$ subunit partitions with $\text{CaV}_2.1$ into lipid rafts in cerebellum: implications for localization and function. *J Neurosci*. 2006; 26:8748–8757. [PubMed: 16928863]
- Davies A, Hendrich J, Van Minh AT, Wratten J, Douglas L, Dolphin AC. Functional biology of the $\alpha_2\delta$ subunits of voltage-gated calcium channels. *Trends Pharmacol Sci*. 2007; 28:220–228. [PubMed: 17403543]
- Day NC, Volsen SG, McCormack AL, Craig PJ, Smith W, Beattie RE, Shaw PJ, Ellis SB, Harpold MM, Ince PG. The expression of voltage-dependent calcium channel beta subunits in human hippocampus. *Brain Res Mol Brain Res*. 1998; 60:259–269. [PubMed: 9757060]
- Deisseroth K, Mermelstein PG, Xia H, Tsien RW. Signaling from synapse to nucleus: the logic behind the mechanisms. *Curr Opin Neurobiol*. 2003; 13:354–365. [PubMed: 12850221]
- Di Biase V, Obermair GJ, Szabo Z, Altier C, Sanguesa J, Bourinet E, Flucher BE. Stable membrane expression of postsynaptic $\text{CaV}1.2$ calcium channel clusters is independent of interactions with AKAP79/150 and PDZ proteins. *J Neurosci*. 2008; 28:13845–13855. [PubMed: 19091974]
- Dietrich D, Kirschstein T, Kukley M, Pereverzev A, von der Brélie C, Schneider T, Beck H. Functional specialization of presynaptic $\text{CaV}2.3$ Ca^{2+} channels. *Neuron*. 2003; 39:483–496. [PubMed: 12895422]
- Doering CJ, Peloquin JB, McRory JE. The $\text{Ca}(v)1.4$ calcium channel: more than meets the eye. *Channels*. 2007; 1:3–10. [PubMed: 19151588]
- Dolmetsch R. Excitation-transcription coupling: signaling by ion channels to the nucleus. *Sci STKE*. 2003; 2003:PE4. [PubMed: 12538881]
- Dolphin AC. Beta subunits of voltage-gated calcium channels. *J Bioenerg Biomembr*. 2003; 35:599–620. [PubMed: 15000522]
- Doyle J, Ren X, Lennon G, Stubbs L. Mutations in the *Cacn11a4* calcium channel gene are associated with seizures, cerebellar degeneration, and ataxia in tottering and leaner mutant mice. *Mamm Genome*. 1997; 8:113–120. [PubMed: 9060410]
- Fletcher TL, De Camilli P, Banker G. Synaptogenesis in hippocampal cultures: evidence indicating that axons and dendrites become competent to form synapses at different stages of neuronal development. *J Neurosci*. 1994; 14:6695–6706. [PubMed: 7965070]
- Gomez-Ospina N, Tsuruta F, Barreto-Chang O, Hu L, Dolmetsch R. The C terminus of the L-type voltage-gated calcium channel $\text{Ca}(V)1.2$ encodes a transcription factor. *Cell*. 2006; 127:591–606. [PubMed: 17081980]
- Green EM, Barrett CF, Bultynck G, Shamah SM, Dolmetsch RE. The tumor suppressor $\text{eIF}3\epsilon$ mediates calcium-dependent internalization of the L-type calcium channel $\text{CaV}1.2$. *Neuron*. 2007; 55:615–632. [PubMed: 17698014]
- Harms KJ, Craig AM. Synapse composition and organization following chronic activity blockade in cultured hippocampal neurons. *J Comp Neurol*. 2005; 490:72–84. [PubMed: 16041714]
- Hell JW, Westenbroek RE, Warner C, Ahljianian MK, Prystay W, Gilbert MM, Snutch TP, Catterall WA. Identification and differential subcellular localization of the neuronal class C and class D L-type calcium channel α_1 subunits. *J Cell Biol*. 1993; 123:949–962. [PubMed: 8227151]
- Hobom M, Dai S, Marais E, Lacinova L, Hofmann F, Klugbauer N. Neuronal distribution and functional characterization of the calcium channel $\alpha_2\delta_2$ subunit. *Eur J Neurosci*. 2000; 12:1217–1226. [PubMed: 10762351]
- Ibata K, Sun Q, Turrigiano GG. Rapid synaptic scaling induced by changes in postsynaptic firing. *Neuron*. 2008; 57:819–826. [PubMed: 18367083]
- Ino M, Yoshinaga T, Wakamori M, Miyamoto N, Takahashi E, Sonoda J, Kagaya T, Oki T, Nagasu T, Nishizawa Y, Tanaka I, Imoto K, Aizawa S, Koch S, Schwartz A, Niidome T, Sawada K, Mori Y. Functional disorders of the sympathetic nervous system in mice lacking the $\alpha_1\text{B}$ subunit ($\text{Cav}2.2$) of N-type calcium channels. *Proc Natl Acad Sci U S A*. 2001; 98:5323–5328. [PubMed: 11296258]

- Jordan BA, Kreutz MR. Nucleocytoplasmic protein shuttling: the direct route in synapse-to-nucleus signaling. *Trends Neurosci.* 2009; 32:392–401. [PubMed: 19524307]
- Jun K, Piedras-Renteria ES, Smith SM, Wheeler DB, Lee SB, Lee TG, Chin H, Adams ME, Scheller RH, Tsien RW, Shin HS. Ablation of P/Q-type Ca(2+) channel currents, altered synaptic transmission, and progressive ataxia in mice lacking the alpha(1A)-subunit. *Proc Natl Acad Sci U S A.* 1999; 96:15245–15250. [PubMed: 10611370]
- Kaech S, Banker G. Culturing hippocampal neurons. *Nat Protoc.* 2006; 1:2406–2415. [PubMed: 17406484]
- Klugbauer N, Lacinova L, Marais E, Hobom M, Hofmann F. Molecular diversity of the calcium channel alpha2delta subunit. *J Neurosci.* 1999; 19:684–691. [PubMed: 9880589]
- Koschak A, Obermair GJ, Pivotto F, Sinnegger-Brauns MJ, Striessnig J, Pietrobon D. Molecular nature of anomalous L-type calcium channels in mouse cerebellar granule cells. *J Neurosci.* 2007; 27:3855–3863. [PubMed: 17409250]
- Leroy J, Richards MW, Butcher AJ, Nieto-Rostro M, Pratt WS, Davies A, Dolphin AC. Interaction via a key tryptophan in the I–II linker of N-type calcium channels is required for beta1 but not for palmitoylated beta2, implicating an additional binding site in the regulation of channel voltage-dependent properties. *J Neurosci.* 2005; 25:6984–6996. [PubMed: 16049174]
- Lorenzon NM, Foehring RC. Characterization of pharmacologically identified voltage-gated calcium channel currents in acutely isolated rat neocortical neurons. I. Adult neurons. *J Neurophysiol.* 1995; 73:1430–1442. [PubMed: 7643158]
- Ludwig A, Flockerzi V, Hofmann F. Regional expression and cellular localization of the alpha1 and beta subunit of high voltage-activated calcium channels in rat brain. *J Neurosci.* 1997; 17:1339–1349. [PubMed: 9006977]
- Mata J, Marguerat S, Bahler J. Post-transcriptional control of gene expression: a genome-wide perspective. *Trends Biochem Sci.* 2005; 30:506–514. [PubMed: 16054366]
- Mochida S, Westenbroek RE, Yokoyama CT, Itoh K, Catterall WA. Subtype-selective reconstitution of synaptic transmission in sympathetic ganglion neurons by expression of exogenous calcium channels. *Proc Natl Acad Sci U S A.* 2003; 100:2813–2818. [PubMed: 12601155]
- Moosmang S, Haider N, Klugbauer N, Adelsberger H, Langwieser N, Muller J, Stuess M, Marais E, Schulla V, Lacinova L, Goebbels S, Nave KA, Storm DR, Hofmann F, Kleppisch T. Role of hippocampal Cav1.2 Ca²⁺ channels in NMDA receptor-independent synaptic plasticity and spatial memory. *J Neurosci.* 2005; 25:9883–9892. [PubMed: 16251435]
- Mori Y, Friedrich T, Kim MS, Mikami A, Nakai J, Ruth P, Bosse E, Hofmann F, Flockerzi V, Furuichi T, et al. Primary structure and functional expression from complementary DNA of a brain calcium channel. *Nature.* 1991; 350:398–402. [PubMed: 1849233]
- Obermair GJ, Kaufmann WA, Knaus HG, Flucher BE. The small conductance Ca²⁺-activated K⁺ channel SK3 is localized in nerve terminals of excitatory synapses of cultured mouse hippocampal neurons. *Eur J Neurosci.* 2003; 17:721–731. [PubMed: 12603262]
- Obermair GJ, Schlick B, Di Biase V, Subramanyam P, Gebhart M, Baumgartner S, Flucher BE. Reciprocal interactions regulate targeting of calcium channel β subunits and membrane expression of α 1 subunits in cultured hippocampal neurons. *J Biol Chem.* 2010; 285:5776–5791. [PubMed: 19996312]
- Obermair GJ, Szabo Z, Bourinet E, Flucher BE. Differential targeting of the L-type Ca²⁺ channel alpha 1C (CaV1.2) to synaptic and extrasynaptic compartments in hippocampal neurons. *Eur J Neurosci.* 2004; 19:2109–2122. [PubMed: 15090038]
- Obermair GJ, Tuluc P, Flucher BE. Auxiliary Ca(2+) channel subunits: lessons learned from muscle. *Curr Opin Pharmacol.* 2008; 8:311–318. [PubMed: 18329337]
- Pichler M, Cassidy TN, Reimer D, Haase H, Kraus R, Ostler D, Striessnig J. Beta subunit heterogeneity in neuronal L-type Ca²⁺ channels. *J Biol Chem.* 1997; 272:13877–13882. [PubMed: 9153247]
- Pravettoni E, Bacci A, Coco S, Forbicini P, Matteoli M, Verderio C. Different localizations and functions of L-type and N-type calcium channels during development of hippocampal neurons. *Dev Biol.* 2000; 227:581–594. [PubMed: 11071776]

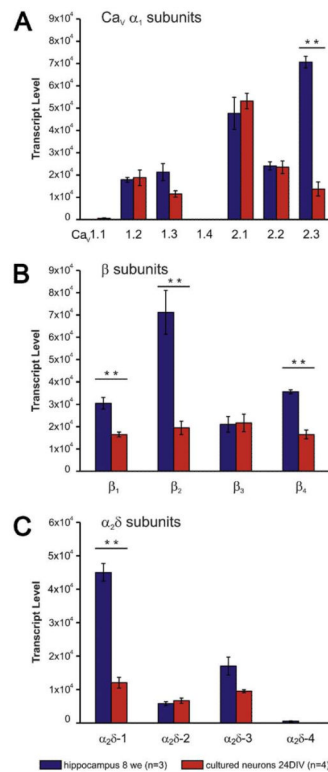
- Qin N, Yagel S, Momplaisir ML, Codd EE, D'Andrea MR. Molecular cloning and characterization of the human voltage-gated calcium channel $\alpha(2)\delta-4$ subunit. *Mol Pharmacol.* 2002; 62:485–496. [PubMed: 12181424]
- Randall A, Tsien RW. Pharmacological dissection of multiple types of Ca^{2+} channel currents in rat cerebellar granule neurons. *J Neurosci.* 1995; 15:2995–3012. [PubMed: 7722641]
- Rao A, Craig AM. Activity regulates the synaptic localization of the NMDA receptor in hippocampal neurons. *Neuron.* 1997; 19:801–812. [PubMed: 9354327]
- Saegusa H, Kurihara T, Zong S, Minowa O, Kazuno A, Han W, Matsuda Y, Yamanaka H, Osanai M, Noda T, Tanabe T. Altered pain responses in mice lacking $\alpha 1E$ subunit of the voltage-dependent Ca^{2+} channel. *Proc Natl Acad Sci U S A.* 2000; 97:6132–6137. [PubMed: 10801976]
- Scholz KP, Miller RJ. Developmental changes in presynaptic calcium channels coupled to glutamate release in cultured rat hippocampal neurons. *J Neurosci.* 1995; 15:4612–4617. [PubMed: 7790927]
- Sinnesger-Brauns MJ, Huber IG, Koschak A, Wild C, Obermair GJ, Einzinger U, Hoda JC, Sartori SB, Striessnig J. Expression and 1,4-dihydropyridine-binding properties of brain L-type calcium channel isoforms. *Mol Pharmacol.* 2009; 75:407–414. [PubMed: 19029287]
- Splawski I, Timothy KW, Sharpe LM, Decher N, Kumar P, Bloise R, Napolitano C, Schwartz PJ, Joseph RM, Condouris K, Tager-Flusberg H, Priori SG, Sanguinetti MC, Keating MT. $\text{Ca}(V)1.2$ calcium channel dysfunction causes a multisystem disorder including arrhythmia and autism. *Cell.* 2004; 119:19–31. [PubMed: 15454078]
- Subramanyam P, Obermair GJ, Baumgartner S, Gebhart M, Striessnig J, Kaufmann WA, Geley S, Flucher BE. Activity and calcium regulate nuclear targeting of the calcium channel $\beta(4b)$ subunit in nerve and muscle cells. *Channels.* 2009; 3:343–355. [PubMed: 19755859]
- Takahashi Y, Jeong SY, Ogata K, Goto J, Hashida H, Isahara K, Uchiyama Y, Kanazawa I. Human skeletal muscle calcium channel $\alpha 1S$ is expressed in the basal ganglia: distinctive expression pattern among L-type Ca^{2+} channels. *Neurosci Res.* 2003; 45:129–137. [PubMed: 12507731]
- Turrigiano GG. The self-tuning neuron: synaptic scaling of excitatory synapses. *Cell.* 2008; 135:422–435. [PubMed: 18984155]
- Turrigiano GG, Nelson SB. Homeostatic plasticity in the developing nervous system. *Nat Rev Neurosci.* 2004; 5:97–107. [PubMed: 14735113]
- Vacher H, Mohapatra DP, Trimmer JS. Localization and targeting of voltage-dependent ion channels in mammalian central neurons. *Physiol Rev.* 2008; 88:1407–1447. [PubMed: 18923186]
- Vandesompele J, De Preter K, Pattyn F, Poppe B, Van Roy N, De Paepe A, Speleman F. Accurate normalization of real-time quantitative RT-PCR data by geometric averaging of multiple internal control genes. *Genome Biol.* 2002; 3 RESEARCH0034.
- Westenbroek RE, Sakurai T, Elliott EM, Hell JW, Starr TV, Snutch TP, Catterall WA. Immunochemical identification and subcellular distribution of the $\alpha 1A$ subunits of brain calcium channels. *J Neurosci.* 1995; 15:6403–6418. [PubMed: 7472404]
- Wu LG, Borst JG, Sakmann B. R-type Ca^{2+} currents evoke transmitter release at a rat central synapse. *Proc Natl Acad Sci U S A.* 1998; 95:4720–4725. [PubMed: 9539805]
- Wu LG, Westenbroek RE, Borst JG, Catterall WA, Sakmann B. Calcium channel types with distinct presynaptic localization couple differentially to transmitter release in single calyx-type synapses. *J Neurosci.* 1999; 19:726–736. [PubMed: 9880593]
- Wycisk KA, Budde B, Feil S, Skosyrski S, Buzzi F, Neidhardt J, Glaus E, Nurnberg P, Ruether K, Berger W. Structural and functional abnormalities of retinal ribbon synapses due to *Cacna2d4* mutation. *Invest Ophthalmol Vis Sci.* 2006; 47:3523–3530. [PubMed: 16877424]
- Yasuda R, Sabatini BL, Svoboda K. Plasticity of calcium channels in dendritic spines. *Nat Neurosci.* 2003; 6:948–955. [PubMed: 12937422]

**Fig. 1.**

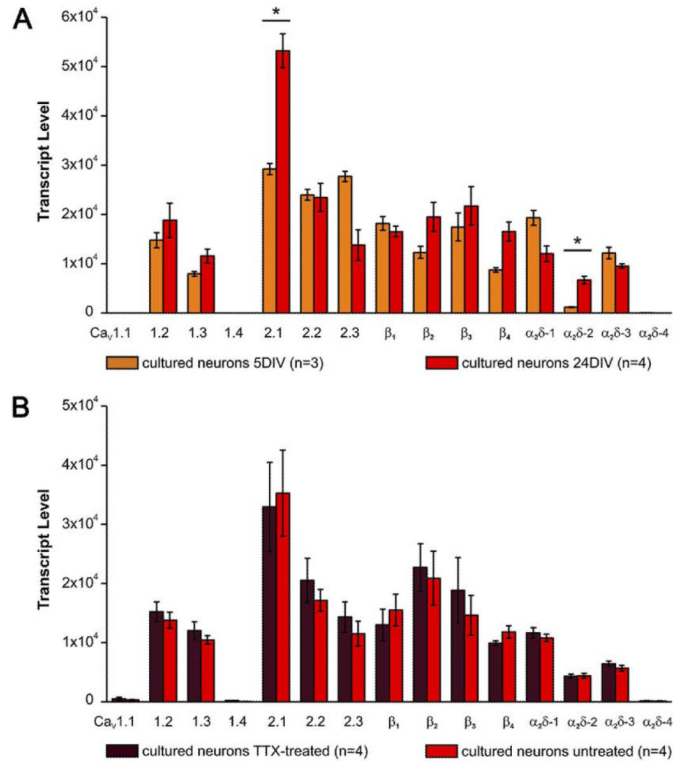
Expression profile of the high voltage-activated Ca²⁺ channel α_1 , β , and $\alpha_2\delta$ subunits in mouse hippocampus, cortex, and cerebellum. (A) Hippocampus (blue), cortex (green), and cerebellum (yellow) express all Ca_v α_1 subunits except Ca_v1.1 and Ca_v1.4. Subunit expression levels in hippocampus and cortex are similar with the exception of Ca_v2.3, which is highest expressed in hippocampus. In cerebellum Ca_v2.1 is the most abundant isoform, Ca_v1.2 is higher and Ca_v1.3 lower than in hippocampus and cortex. Ca_v2.2 is uniformly expressed in all three brain regions. (B) mRNA of all four β subunits is present in hippocampus, cortex, and cerebellum. β_2 and β_4 are the dominant isoforms in hippocampus and cerebellum, respectively. In cortex β subunits are expressed at similar levels. (C) $\alpha_2\delta$ -1 is the major $\alpha_2\delta$ isoform in hippocampus and cortex, whereas in cerebellum it is $\alpha_2\delta$ -2. Levels of $\alpha_2\delta$ -3 are uniform throughout the brain regions tested. Compared to the other auxiliary subunits $\alpha_2\delta$ -4 expression levels were negligible, although above the limit of quantification in all qRT-PCR runs. * $P < 0.05$; ** $P < 0.01$; 2-way ANOVA plus post hoc ANOVA with Holm correction; error bars: \pm SEM.

**Fig. 2.**

Developmental changes of Ca_v subunit mRNA expression in cortex and hippocampus. Ca_v subunit expression profiles were determined in embryonic (E16), postnatal (PD1), and 2 and 8 weeks old BALB/c mice. (A) During development cortical mRNA levels of Ca_v1.2, Ca_v2.2, Ca_v2.3, β₁, β₃, and α₂δ-2 significantly decline, whereas levels of β₂ and β₄ increase. Levels of Ca_v1.3, Ca_v2.1, and α₂δ-1 and α₂δ-3 remain stable. (B) In hippocampus the overall developmental changes are less striking than in cortex. However, the increase in β₂ and the significant drop of β₃ levels between E16 and PD1 are more pronounced. In contrast to whole cortex, levels of Ca_v2.3 did not decline. Although total mRNA levels are negligible in comparison with the other α₂δ subunits, expression of α₂δ-4 increases ~20-fold during development. * *P*<0.05; ** *P*<0.01; 2-way ANOVA plus post hoc ANOVA with Holm correction; error bars: ±SEM.

**Fig. 3.**

Expression profile of high voltage-activated Ca²⁺ channel α₁, β, and α₂δ subunits in differentiated cultured hippocampal neurons (24 DIV). (A) The majority of α₁ subunits show similar expression levels in the cultured neurons as in 8 weeks old hippocampus. However, expression of Ca_v2.3 was 5-fold lower in cultured neurons. (B) In cultured neurons all β isoforms are expressed at equal amounts, but at significantly lower levels than in hippocampus. (C) α₂δ subunits are expressed at equal amounts and generally lower levels than in hippocampal tissue. α₂δ-4 levels were analyzed separately in five DIV and 24 DIV old neurons (cf. Fig. 4 and Suppl. Fig. 2), but always below detectability. ** *P*<0.01; 2-way ANOVA plus post hoc *t*-test with Holm correction; error bars: ±SEM.

**Fig. 4.**

Effects of development and neuronal activity on Ca_v subunit expression in cultured hippocampal neurons. (A) The majority of Ca_v isoforms shows a slight increase in transcript levels between 5 and 24 DIV. This increase is most obvious for Ca_v2.1, α₂δ-2, and β₄. In contrast to the overall trend, amounts of Ca_v2.3 and α₂δ-1 transcripts decrease during *in vitro* development. (B) Blocking electrical activity by TTX for 24 h did not alter the expression level of any Ca_v subunit isoform. * $P < 0.05$; 2-way ANOVA plus post hoc *t*-test with Holm correction; error bars: ±SEM.

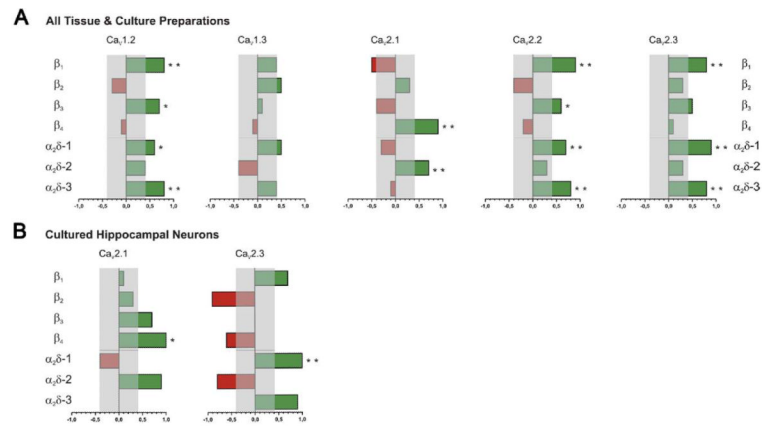


Fig. 5. Correlation analysis of $\text{Ca}_V \alpha_1$ subunit expression with individual β and $\alpha_2\delta$ isoforms. Correlation coefficients were calculated between the transcript amounts of the individual α_1 and the auxiliary β and $\alpha_2\delta$ subunits including measurements from all tissue and culture preparations. The abscissa represents the size and direction of the correlation coefficients whereby direct (positive) and indirect (negative) coefficients are indicated by green and red bars, respectively. Asterisks mark significant correlations and the gray area indicates the cut-off ($r=0.4$) for weak correlations. (A) Correlation analysis clearly identified the previously demonstrated association of the $\text{Ca}_V2.1 \alpha_1$ subunit with β_4 and $\alpha_2\delta-2$. Interestingly, $\text{Ca}_V1.2$, $\text{Ca}_V2.2$, and $\text{Ca}_V2.3$ showed similar degrees of correlations with the same set of β and $\alpha_2\delta$ subunits. Expression of $\text{Ca}_V1.3$ did not reveal a strong correlation with any auxiliary subunit. (B) Similar correlation coefficients were identified for $\text{Ca}_V2.1$ and $\text{Ca}_V2.3$ by including only the measurements from cultured hippocampal neurons. * $P<0.05$; ** $P<0.01$; Pearson correlation.

Table 1

TaqMan gene expression assays for all high-voltage activated Ca²⁺ channel α_1 , β , and $\alpha_2\delta$ subunits

Subunit	GenBank accession	Assay ID	Exon boundary	Intron length (bp)
Ca _v 1.1	NM_014193	Mm00489257_m1	9–10	1768
Ca _v 1.2	NM_009781	Mm00437917_m1	8a–9	7241
Ca _v 1.3	NM_028981	Mm01209919_m1	29–30	5412
Ca _v 1.4	NM_019582	Mm00490443_m1	18–19	541
Ca _v 2.1	NM_007578	Mm00432190_m1	40–41	3281
Ca _v 2.2	NM_007579	Mm00432226_m1	38–39	2530
Ca _v 2.3	NM_009782	Mm00494444_m1	43–44	4240
β_1	NM_031173	Mm00518940_m1	1–2	2575
β_2	NM_023116	Mm00659092_m1	13–14	1148
β_3	NM_007581	Mm00432233_m1	1–2	4274
β_4	NM_146123	Mm00521623_m1	11–12	12,878
$\alpha_2\delta$ -1	NM_009784	Mm00486607_m1	33–34	2583
$\alpha_2\delta$ -2	NM_020263	Mm00457825_m1	1–2	25,769
$\alpha_2\delta$ -3	NM_009785	Mm00486613_m1	5–6	44,477
$\alpha_2\delta$ -4	NM_001033382	Mm01190105_m1	8–9	2407

Table 2

cDNA specific primer sequences for standard template amplification

	Forward primer	Reverse primer	Fragment size (bp)
C _v 1.1	5'-gttacatgagctggatcacacag-3'	5'-atgagcatttcgatggaag-3'	349
C _v 1.2	5'-atgccaaagcctatgggtat-3'	5'-caggtagccttggagatctcttc-3'	201
C _v 1.3	5'-acattctgaacatggcttcacag-3'	5'-aggacttgaigaaggtccacag-3'	327
C _v 1.4	5'-ctcttctctctggaactacatc-3'	5'-gtaccacctctctctgggtacta-3'	324
C _v 2.1	5'-ggtcacaccacaaagtcac-3'	5'-ccagctctctggaacatctctg-3'	306
C _v 2.2	5'-cacttagaacgaattcctgagct-3'	5'-tatcatgagagcagcatgacctt-3'	408
C _v 2.3	5'-aaggtaaagaacaagacagcag-3'	5'-gtctgtaccaccaccagagatgttg-3'	267
β_1	5'-gaicctctccatggtccagaa-3'	5'-ctgacctctcttaaggcttc-3'	266
β_2	5'-gactatctggagcctactctgaaag-3'	5'-ctctcttgggttcagagatcaaa-3'	317
β_3	5'-cccatgtagacgactctctacg-3'	5'-acagtagctgacatgggtctcac-3'	216
β_4	5'-gctgattaaagctccagagaaagtc-3'	5'-tctctcctctgactctgtaaat-3'	288
$\alpha_2\delta$ -1	5'-gcatgtagacaccctggttaata-3'	5'-acagctccagtaaacaccactgaaatga-3'	347
$\alpha_2\delta$ -2	5'-ccgctctctctctctg-3'	5'-cttctctccagcagctct-3'	273
$\alpha_2\delta$ -3	5'-gtaataactcaatgctgctg-3'	5'-attaatcccctgggtactgctctga-3'	305
$\alpha_2\delta$ -4	5'-cactatcccnaagacatct-3'	5'-caagggaagctctctctccaccag-3'	337

Table 3
Properties of standard curves and limits of detection (LOD) and quantification (LOQ)

	B	SE-B ^a	Y-int. ^b	SE-Y ^a	R ²	LOD ^c	LOQ ^d
Ca _v 1.1	-3.449	0.028	38.02	0.13	0.998	3	15
Ca _v 1.2	-3.648	0.023	38.54	0.11	0.998	37	142
Ca _v 1.3	-3.692	0.043	41.14	0.19	0.995	60	78
Ca _v 1.4	-3.420	0.029	37.41	0.13	0.997	5	34
Ca _v 2.1	-3.556	0.043	38.36	0.20	0.995	4	102
Ca _v 2.2	-3.497	0.053	37.86	0.25	0.993	5	155
Ca _v 2.3	-3.506	0.040	37.23	0.18	0.995	4	59
β_1	-3.474	0.037	36.34	0.17	0.995	3	34
β_2	-3.491	0.048	39.48	0.22	0.989	6	190
β_3	-3.520	0.039	37.58	0.18	0.993	12	114
β_4	-3.535	0.050	38.01	0.23	0.992	5	137
$\alpha_2\delta$ -1	-3.436	0.058	36.80	0.27	0.990	5	127
$\alpha_2\delta$ -2	-3.572	0.036	38.07	0.17	0.997	22	117
$\alpha_2\delta$ -3	-3.533	0.035	37.88	0.16	0.994	4	59
$\alpha_2\delta$ -4	-3.412	0.028	37.70	0.13	0.996	3	27

^aSE-B, -Y, standard error of B and Y intercept, respectively.

^bY-int., Y-intercept (Ct value).

^cLOD, limit of detection (number of transcripts).

^dLOQ, limit of quantification (number of transcripts).

Table 4

Number of mRNA molecules in a single cultured hippocampal neuron

Ca _v subunit	Number of transcript molecules
Ca _v 1.1	0.0
Ca _v 1.2	5.0
Ca _v 1.3	2.2
Ca _v 1.4	0.0
Ca _v 2.1	11.2
Ca _v 2.2	5.4
Ca _v 2.3	2.3
β_1	3.6
β_2	4.2
β_3	4.4
β_4	3.8
$\alpha_2\delta$ -1	2.3
$\alpha_2\delta$ -2	1.8
$\alpha_2\delta$ -3	2.1
$\alpha_2\delta$ -4 ^a	0.0

Calculations are based on the qRT-PCR experiment on cultured hippocampal neurons (24 DIV) with highest RNA yield.

^aThe assay for $\alpha_2\delta$ -4 was not included in the same qRT-PCR experiments. However, in other qRT-PCR runs on cultured hippocampal neurons $\alpha_2\delta$ -4 levels were always below detectability (cf. Fig. 4 and Suppl. Fig. 2).